Osmotic-pressure-induced phase transition of a surfactant-DNA complex

S. Madhukar●, A. V. Radhakrishnan,[*] and V. A. Raghunathan[†]

Raman Research Institute, Bangalore 560 080, India

We have studied the effect of osmotic pressure on complexes formed by DNA with the cationic surfactant cetyltrimethylammonium tosylate using small-angle x-ray scattering. Earlier studies have shown that these complexes exhibit three different phases depending on the DNA and surfactant concentrations in the solution. The hexagonal superlattice phase ($H_{I,s}^c$) is found to be corralled into the hexagonal phase (H_I^c) above a threshold osmotic pressure. We have also estimated the DNA to surfactant micelle stoichiometry of the complexes in the three phases using elemental analysis. Our results provide further support for the structures of these complexes proposed earlier based on small-angle x-ray scattering data.

I. INTRODUCTION

A significant fraction of the counterions of a highly charged macroion, dispersed in an aqueous medium, condense onto it, resulting in an effective charge density much lower than that expected from its chemical structure [1,2]. In systems composed of oppositely charged macroions, complexation occurs mainly due to the gain in entropy achieved through the release of the bound counterions from the two constituents [3,4]. In the case of highly flexible polyelectrolytes these complexes form a liquid coacervate [5]. On the other hand, if, at least, one of the two species is sufficiently rigid, complexes characterized by long-range orientational and translational order are observed [6–13].

Complexes of DNA with cationic lipids and surfactants have been widely studied due to their potential application in gene delivery and their interesting electrostatics [14–17]. Complexes of DNA with bilayer forming cationic lipids exhibit a lamellar structure where the DNA strands are sandwiched between the bilayers [6,7]. This structure is transformed into an inverted hexagonal structure on decreasing the bending rigidity of the bilayer or on decreasing its spontaneous curvature [8]. This transition can also be driven by applying an osmotic pressure to the complex using a water soluble neutral polymer [18]. In the case of single chain cationic surfactants that self-assemble into cylindrical micelles, the complexes have a two-dimensional structure with the long axes of the DNA and micelles oriented normal to the plane of the lattice [19]. The structure of these complexes is found to be very sensitive to the nature of the surfactant counterion [13]. For example, complexes of DNA with cetyltrimethylammonium bromide (CTAB) show a two-dimensional close-packed intercalated hexagonal structure [19]. On the other hand, in the

case of cetyltrimethylammonium tosylate (CTAT), containing the strongly binding tosylate counterion, three different two-dimensional structures are observed, depending on the DNA and surfactant concentrations in the solution [13]. CTAT is known to self-assemble into wormlike micelles (WLM) at concentrations as low as 1 wt % in water, which mimic the behavior of polyelectrolytes in many ways [20,21] and ordered liquid crystalline phases at higher concentrations [22]. The ability of CTAT to form WLM, and the competition between the tosylate counterion and DNA to bind to the micelle are believed to be responsible for the observed polymorphism of these complexes [13].

The three structures observed in CTAT-DNA complexes are schematically shown in Fig. 1, and their small-angle x-ray scattering (SAXS) patterns are given in Fig. 2. The square lattice (S_I^c) is seen at a high surfactant to the DNA base molar ratio (ρ). Assuming each DNA strand and surfactant micelle to be infinitely long, this structure has a 1:1 DNA to micelle stoichiometry. The intercalated hexagonal structure (H_I^c) occurs at low values of both ρ and surfactant concentration C_s. This is the only structure exhibited by CTAB-DNA complexes [19]. The DNA to micelle stoichiometry in this phase is 2:1. A hexagonal phase with a much higher lattice parameter ($H_{I,s}^c$) than H_I^c occurs at low ρ and higher C_s. Structural models for these three phases of CTAT-DNA complexes have been proposed in Ref. [13], based on a detailed analysis of small-angle x-ray scattering data. Since S_I^c and H_I^c have two-dimensional close-packed structures, their lattice parameters have specific relationships with the radii of the surfactant micelle (r_m) and DNA (r_d), given by $a_S = \sqrt{2}(r_m + r_d)$ and $a_H = \sqrt{3}(r_m + r_d)$. Typical values of a_S and a_H are 5.0 and 6.0 nm, respectively, and taking the radius of a hydrated DNA to be 1.25 nm [6], the radius of the micelle turns out to be about 2.25 nm, which is in good agreement with the value of 2.15 nm obtained from neutron scattering experiments [23]. Thus, the observed values of a_S and a_H are consistent with the proposed closed-packed structures of these two phases. This conclusion is supported by the detailed analysis of the diffraction data

---

[*]Present address: Interdisciplinary Institute for Neuroscience, UMR 5297- CNRS/Universite de Bordeaux, 146, Rue Leo Saignat, Bordeaux 33077, France.

[†]varaghu@rri.res.in

FIG. 2. Typical SAXS patterns of the hexagonal (H_I^c), super-hexagonal ($H_{I,s}^c$), and square (S_I^c) phases of CTAT-DNA complexes. Peaks in the scattering patterns of H_I^c and $H_{I,s}^c$ can be indexed following the scheme $q_{hk} \propto \sqrt{h^2 + k^2 + hk}$, whereas those in the scattering pattern of S_I^c can be indexed following the scheme $q_{hk} \propto \sqrt{h^2 + k^2}$. Note that the (1,0) peak is always absent in the case of $H_{I,s}^c$.
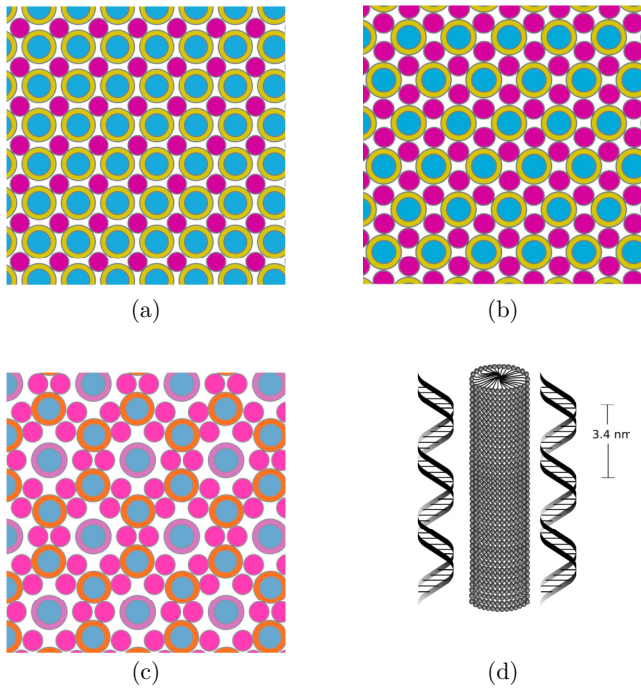
FIG. 1. Schematic of different two-dimensional structures observed in CTAT-DNA complexes. The smaller disks correspond to DNA strands, and the larger ones correspond to cylindrical surfactant micelles with an inner hydrocarbon core surrounded by the head-group region. (a) Close-packed square lattice (S_I^c), (b) close-packed hexagonal lattice (H_I^c), and (c) swollen hexagonal superlattice ($H_{I,s}^c$). The DNA to micelle stoichiometry in (a) is 1:1, whereas it is 2:1 in both (b) and (c). Parallel arrangement of the DNA strand and micelle along the direction normal to the plane of the lattice is depicted in (d).

from these structures presented in Ref. [13]. Furthermore, as mentioned above, the formation of these two phases can be rationalized in terms of the competition between DNA and the surfactant counterion to bind to the micelle. The structure and stability of the third phase are, however, more difficult to account for. Its structure ($H_{I,s}^c$) corresponds to a slightly swollen $\sqrt{3} \times \sqrt{3}$ superlattice of H_I^c. Such a superlattice structure has not been reported in any other macroion complexes hitherto. Since it is not a closed-packed structure, its lattice parameter cannot be deduced from the DNA and micellar diameters. Moreover, energetics of these systems have not been studied in any detail until now and, hence, it is not clear as to why this structure is preferred over the H_I^c at higher values of C_s.

Diffraction patterns of CTAT-DNA complexes contain only a very limited number of peaks as in the case of most soft matter systems. Hence, it is important to test the structures derived from these data using alternative experimental techniques. Since the proposed $H_{I,s}^c$ structure is a slightly swollen version of H_I^c, it can be expected to transform into the latter on application of an osmotic pressure. Such osmotic pressure induced structural changes have been widely studied in many soft materials, including lipid membranes [24–26] and macroion complexes [12,18]. With this motivation, we have studied the stability of the three phases of CTAT-DNA
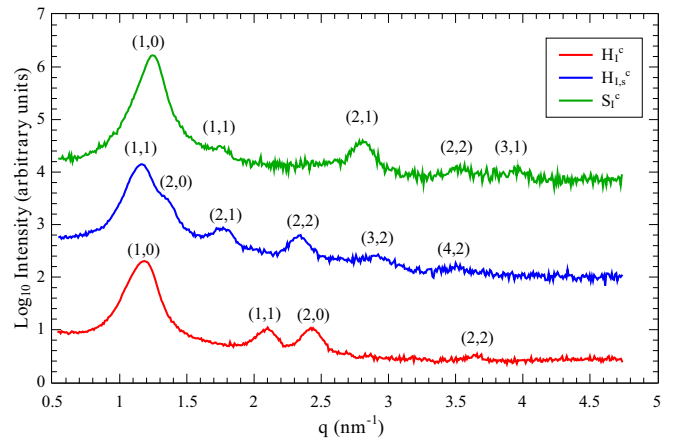
complexes under an osmotic pressure applied using a neutral water soluble polymer. We find that the $H_{I,s}^c$ phase can be converted into H_I^c above a threshold osmotic pressure. No such transformation is observed in the other two cases. In all three cases a disordered structure is observed at the highest osmotic pressure used. The observed transformation of the $H_{I,s}^c$ structure into H_I^c is consistent with their proposed structures. We have also determined the DNA to surfactant stoichiometry in the three phases using elemental analysis. The values obtained are in fair agreement with those estimated from the proposed structures of the three phases. This paper, thus, provides further confirmation of the structures of these complexes determined from their small-angle x-ray scattering data.

II. EXPERIMENTAL SECTION

CTAT, sodium salt of calf thymus DNA, polyethylene glycol of molecular weight 8000 (PEG 8000), and polyvinylpyrrolidone of molecular weight 10 000 (PVP10 000) were obtained from Sigma-Aldrich. All chemicals were used as received. Complexes were prepared at different points on the ρ-C_s plane, spanning the three phases, where ρ is the surfactant to DNA base molar ratio and C_s is the surfactant concentration, by adding appropriate amounts of DNA to surfactant solutions in deionized water (Millipore). Samples were equilibrated for about a week. In these samples the complexes are suspended in an aqueous solution of the released counterions and either excess DNA or surfactant, depending on the chosen value of ρ.

For the osmotic pressure experiments samples were prepared at selected CTAT and DNA concentrations as described above and were equilibrated for about a week. These samples contain dense, gel-like complexes that are suspended in an aqueous solution. Appropriate amounts of PEG8000 or PVP10 000 were added to the supernatant in order to get the desired final polymer concentration

TABLE I. Effect of osmotic pressure, applied using PEG8000 on the structure of CTAT-DNA complexes.

Complex		Lattice parameter (nm) at wt % of PEG8000						
ρ	C_s (mM)	0%	2.5%	5%	7.5%	10%	15%	20%
0.5	50	6.10 (H_I^c)	6.02 (H_I^c)	5.97 (H_I^c)	5.88 (H_I^c)	5.80 (H_I^c)	5.80 (H_I^c)	5.80 (H_I^c)
0.5	100	10.81 ($H_{I,s}^c$)	10.81 ($H_{I,s}^c$)	6.05 (H_I^c)	6.01 (H_I^c)	5.91 (H_I^c)	5.83 (H_I^c)	5.83 (H_I^c)
1	150	10.77 ($H_{I,s}^c$)	10.74 ($H_{I,s}^c$)	10.74 ($H_{I,s}^c$)	6.05 (H_I^c)	5.94 (H_I^c)	5.94 (H_I^c)	5.83 (H_I^c)
2	100	5.05 (S_I^c)	5.05 (S_I^c)	4.97 (S_I^c)	4.97 (S_I^c)	4.97 (S_I^c)	4.82 (S_I^c)	4.82 (S_I^c)

in the aqueous medium. The samples were then sealed and left to equilibrate for 10 more days. This sample preparation protocol is similar to that used in Ref. [18]. The polymer solution forms a separate phase coexisting with the complex and, hence, applies an osmotic pressure on it. Values of the osmotic pressure exerted by solutions of these two polymers, taken from the literature, are given in Appendix C. For diffraction studies, the complex along with some supernatant was taken in glass capillaries, which were then flame sealed to avoid any loss of water. Small-angle x-ray scattering data, covering a range of scattering vector (q) from 0.01 to 5.0 nm^{-1}, were collected using a Hecus S3-Micro system, fitted with a one-dimensional position-sensitive detector. Typical exposure time was 30 min. Data were collected again from these samples after about a week to ensure equilibration.

Elemental analysis was conducted using a vario MICRO cube CHNS elemental analyzer (Elementar). For our experiments complexes were made at the desired values of ρ and C_s and the entire amount of the complex was transferred to tin boats, postequilibration. The samples were then dried thoroughly by placing in an evacuated desiccator for 3 days. They were then weighed and crimped immediately to avoid rehydration.

The C, N, and S contents of the complexes were obtained from elemental analysis. Weight fractions of the different elements acquired from the experiment were converted into molar fractions using their atomic weights. The total number of carbon, nitrogen, and sulfur atoms in the complex are given by

$$N_C = C^s n_s + C^b n_b + C^c n,$$
$$N_N = N^s n_s + N^b n_b, \qquad (1)$$
$$N_S = S^c n_c,$$

here, C^s, C^b, and C^c are the numbers of carbon atoms in a surfactant ion, a DNA base, and a counterion, respectively. N^s and N^b are the numbers of nitrogen atoms in a surfactant ion and a DNA base, respectively. S^c is the number of sulfur atoms in a couterion. n_s, n_b, and n_c are the total numbers of surfactant ions, DNA bases, and counterions in the sample, respectively. Calf thymus DNA is known to have a ratio of 41.9% of A-T base pairs and 58.1% of G-C base pairs [27], giving $C^b = 9.79$ and $N^b = 3.71$. The CTA$^+$ surfactant ion and tosylate counterion have the chemical formulas $C_{19}H_{42}N$ and $C_7H_7O_3S$, respectively. Thus, $C^s = 19$, $C^c = 7$, $N^s = 1$, and $S^c = 1$. Hence n_s, n_b, and n_c can be deter-

mined from the values of N_C, N_N, and N_s obtained from the experiment.

III. RESULTS AND DISCUSSION

A. Effect of osmotic pressure

The effect of osmotic pressure on the structure of CTAT-DNA complexes, applied using PEG8000, is summarized in Table I. The corresponding SAXS patterns are given in Fig. 3 and in Appendixs A and B.
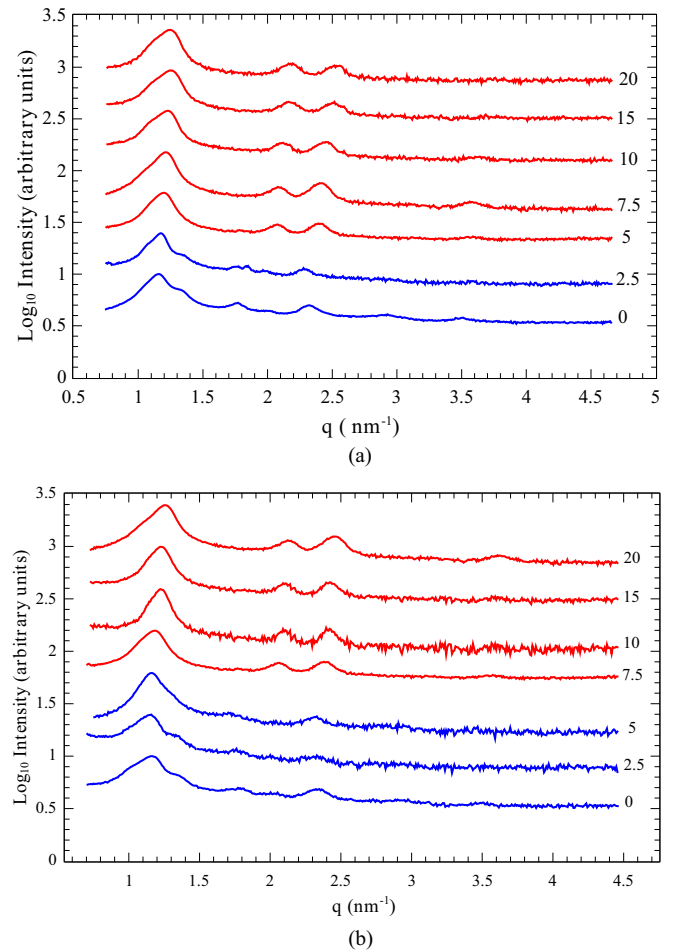

(a)

(b)

FIG. 3. SAXS patterns showing the effect of osmotic pressure on $H_{I,s}^c$. Numbers against the curves indicate the concentration of PEG8000 in the solution. (a) $\rho = 0.5$, [CTAT] = 100 mM. (b) $\rho = 1.0$, [CTAT] = 150 mM.

TABLE II. Effect of osmotic pressure, applied using PVP10 000 on the structure of CTAT-DNA complexes.

	Complex			Lattice parameter (nm) at wt % of PVP10 000			
ρ	C_s (mM)	0%	2%	5%	7.5%	10%	15%
0.5	50	6.07 (H_I^c)	5.97 (H_I^c)	5.83 (H_I^c)	5.73 (H_I^c)	5.73 (H_I^c)	
0.5	100	10.81 ($H_{I,s}^c$)	6.10 (H_I^c)	5.83 (H_I^c)	5.83 (H_I^c)	5.70 (H_I^c)	
1	150	10.70 ($H_{I,s}^c$)	6.07 (H_I^c)	5.88 (H_I^c)	5.73 (H_I^c)	5.73 (H_I^c)	
2	100	5.05 (S_I^c)	4.94 (S_I^c)	4.82 (S_I^c)	4.82 (S_I^c)	4.82 (S_I^c)	

At low osmotic pressures, the $H_{I,s}^c$ structure prepared at $\rho = 0.5$ and $C_s = 100$ mM shows no discernible change with the lattice parameter a remaining at 10.81 nm. However, increasing PEG8000 concentration to 5 wt % converts it into H_I^c with $a = 6.05$ nm [Fig. 3(a)]. A further increase in polymer concentration, up to 20 wt %, induces no change in the structure, but a decrease in the lattice parameter is seen from 6.05 to 5.83 nm as the polymer concentration is increased from 5 to 20 wt %.

For the $H_{I,s}^c$ complex at $\rho = 1$ and $C_s = 150$ mM, the transformation to H_I^c takes place at a higher polymer concentration of 7.5 wt % [Fig. 3(b)]. A further increase in osmotic pressure only causes a change in the lattice parameter of the H_I^c from 6.05 to 5.83 nm between 10 and 20 wt % of PEG8000.

Samples prepared in the H_I^c phase do not show any change in structure (SAXS data given in Appendix A). The lattice parameter changes slightly from 6.10 to 5.80 nm between 0 to 20 wt % of PEG8000. The square phase S_I^c also shows only a change in the lattice parameter across the entire range of pressures applied, from 5.05 nm at 0 wt % to 4.82 nm at 20 wt % (SAXS data given in Appendix B).

The effect of osmotic pressure, applied using PVP10 000 on CTAT-DNA complexes is presented in Table II. The corresponding diffraction patterns are given in Fig. 4 and in Appendixs A and B. As in the case of PEG8000, the $H_{I,s}^c$ phase is found to transform into H_I^c above a threshold concentration of PVP10 000. No structural changes in the H_I^c and S_I^c phases are observed up to a PVP10 000 concentration of 10 wt %. However, in all the three cases a disordered structure is found at 15 wt % of PVP10 000, which gives rise to a very broad peak in the diffraction pattern. The reason for the observed disordering is not currently understood. Interestingly, a similar broadening of diffraction peaks on application of an osmotic pressure has been reported in high density DNA mesophases, which has been attributed to angular frustrations of the DNA molecules imposed by the interaction potential [28]. It is not clear how the presence of cylindrical CTAT micelles in between the DNA in the complexes affects the angular correlations between the DNA. Further work is needed to ascertain if the mechanism proposed in Ref. [28] is applicable to the complexes studied here.

B. Elemental analysis

Elemental analysis of CTAT-DNA complexes at different values of ρ and C_s was carried out. The results are presented in Table III. Here ρ is the surfactant to the DNA base molar
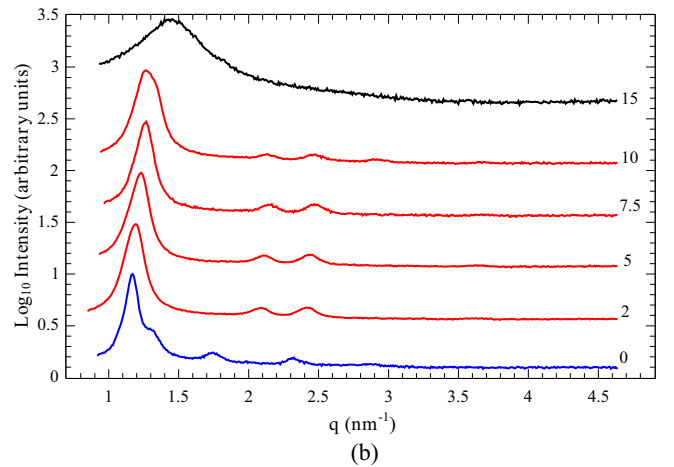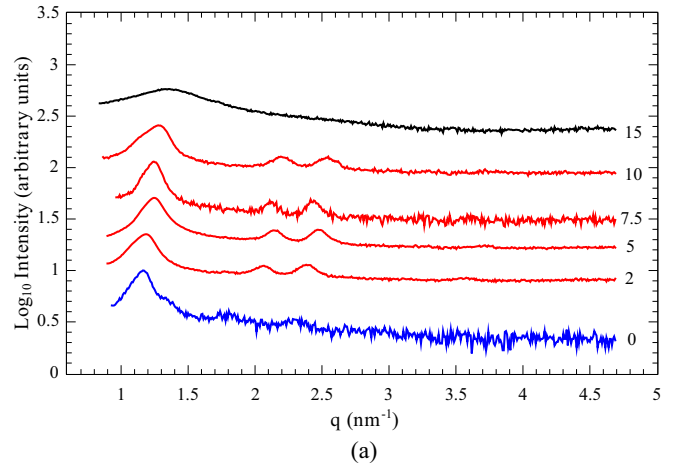

FIG. 4. SAXS patterns showing the effect of osmotic pressure on $H_{I,s}^c$. Numbers against curves indicate the concentration of PVP10 000 in the solution. (a) $\rho = 0.5$, [CTAT] = 100 mM. (b) $\rho = 1.0$, [CTAT] = 150 mM.

TABLE III. Elemental analysis data of CTAT-DNA complexes.

Phase	ρ	C_s (mM)	N (wt %)	C (wt%)	S (wt %)	ρ_c
H_I^c	0.5	50	7.41	49.43	2.63	1.22
	1	50	7.25	49.56	2.61	1.28
$H_{I,s}^c$	0.5	100	6.54	50.33	3.87	1.40
	1	100	6.81	53.49	3.46	1.61
	1	150	7.44	56.20	3.69	1.47
S_I^c	2	100	5.73	58.07	3.75	2.86
	3	50	5.6	59.68	3.58	3.45

ratio in the whole sample and ρ_c ($= n_s/n_b$) is its value in the complex, estimated from the data. Complexes in the H_I^c phase have ρ_c values of about 1.2 to 1.3, whereas those in the $H_{I,s}^c$ phase give values in the range of 1.4–1.6. Values obtained in the S_I^c phase range from 2.9 to 3.5.

Structures of the S_I^c and H_I^c phases, derived from their electron density maps, are close packed and differ in the coordination numbers of the two species (Fig. 1) [13]. In S_I^c each micelle is surrounded by four DNA strands, and each DNA strand is surrounded by four micelles. On the other hand, in H_I^c each micelle is surrounded by six DNA strands, and each DNA strand is surrounded by three micelles. Since these are close-packed structures, they can be expected to be resilient to moderate osmotic pressures as observed. In contrast, structure of the $H_{I,s}^c$ phase is not close packed. It is a slightly swollen version of the H_I^c structure due to the higher concentration of the released counterions in the solution. But instead of swelling uniformly, the tendency of the two oppositely charged species to be in close proximity seems to lead to the superlattice structure with two different types of local micellar environments. Application of osmotic stress on this structure will draw out water from it and can be expected to convert it to the H_I^c structure as observed here. The fact that the value of the lattice parameter of the resulting H_I^c phase is the same as that of the H_I^c phase occurring at lower values of C_s at zero osmotic pressure confirms that they have the same structure. The lower concentration of PVP10 000 needed to drive this transition is a reflection of the higher osmotic pressure exerted by it compared to PEG8000 at similar concentrations (Appendix C). The threshold osmotic pressure for the $H_{I,s}^c \rightarrow H_I^c$ transition in all cases is on the order of 1.0×10^5 Pa, which is about two orders of magnitude lower than that required to transform lamellar lipid-DNA complexes into the inverted hexagonal phase [18]. The much lower value of the threshold osmotic pressure for the $H_{I,s}^c \rightarrow H_I^c$ transition results from the close similarity of the structures of these two phases.

Values of ρ_c ($= n_s/n_b$) in the complexes can be estimated from the structural details of CTAT micelles and B-DNA. The headgroup area of the quaternary ammonium surfactant in the micellar phase is about 0.65 nm^2 [29]. Assuming both the DNA and the micelle to be infinitely long, the S_I^c structure has a DNA to surfactant stoichiometric ratio of 1:1 as can be seen from Fig. 1(a). Taking the micellar radius to be 2.0 nm, the area on the micellar surface corresponding to the height of a base pair along the DNA strand (0.332 nm [27]) turns out to be 4.17 nm^2. This corresponds to about 3.2 surfactant molecules for every DNA base. Hence, $\rho_c \sim 3.2$ in the S_I^c phase. In the $H_{I,s}^c$ and H_I^c structures the DNA to micelle stoichiometric ratio is 2:1 [Figs. 1(b) and 1(c)]. Hence, in these cases $\rho_c \sim 1.6$. The agreement between the estimated and the observed values is fairly good in all the three phases and gives further support to the proposed structures of these phases.

IV. CONCLUSIONS

We have studied the influence of osmotic pressure on the different structures formed by CTAT-DNA complexes. We observe a $H_{I,s}^c \rightarrow H_I^c$ transformation above a threshold value

of the osmotic pressure, which is on the order of 1.0×10^5 Pa. We have also estimated the DNA to micelle stoichiometry in the three phases using elemental analysis. Results of these studies provide further support for the structures of these complexes proposed in Ref. [13], based on x-ray diffraction data. We hope our studies will motivate detailed theoretical investigations into the structural polymorphism of these model systems.

APPENDIX A: EFFECT OF OSMOTIC PRESSURE ON THE H_I^c PHASE
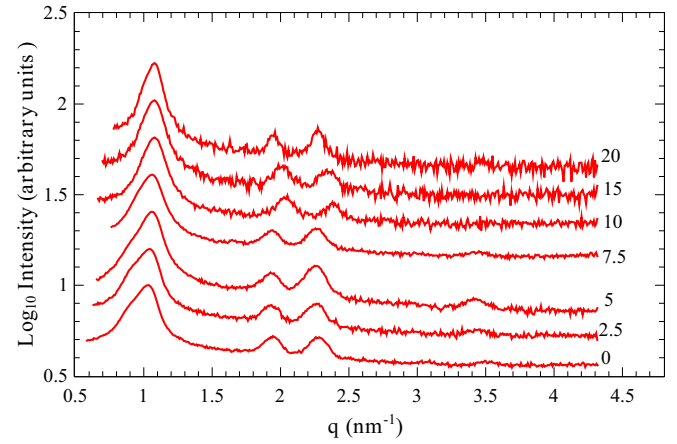
See the SAXS data presented in Figs. 5 and 6.

FIG. 5. SAXS patterns showing the effect of osmotic pressure on H_I^c; $\rho = 0.5$, [CTAT] = 50 mM. Numbers against the curves indicate the concentration of PEG8000 in the solution. Peaks in the scattering patterns can be indexed following the scheme $q_{hk} \propto \sqrt{h^2 + k^2 + hk}$.
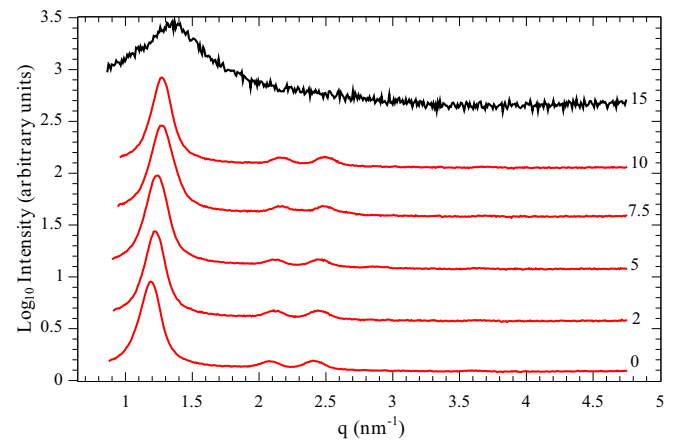

FIG. 6. SAXS patterns showing the effect of osmotic pressure on H_I^c; $\rho = 0.5$, [CTAT] = 50 mM. Numbers against the curves indicate the concentration of PVP10 000 in the solution. Peaks in the scattering patterns can be indexed following the scheme $q_{hk} \propto \sqrt{h^2 + k^2 + hk}$.

APPENDIX B: EFFECT OF OSMOTIC PRESSURE ON THE S_I^c PHASE

See the SAXS data presented in Figs. 7 and 8.

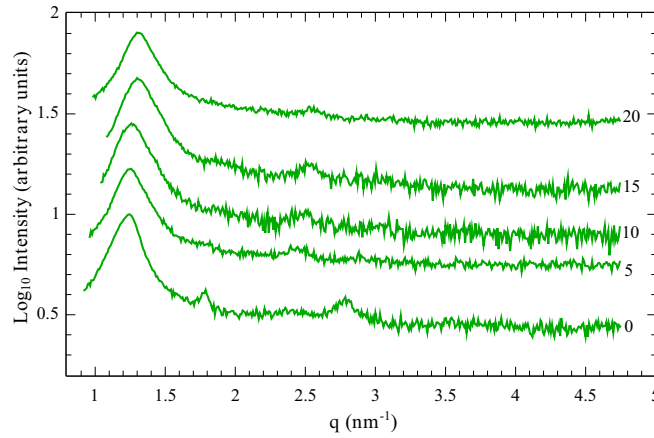

FIG. 7. SAXS patterns showing the effect of osmotic pressure on S_I^c; $\rho = 2$, [CTAT] = 100 mM. Numbers against the curves indicate the concentration of PEG8000 in the solution. Peaks in the scattering patterns can be indexed following the scheme $q_{hk} \propto \sqrt{h^2 + k^2}$.
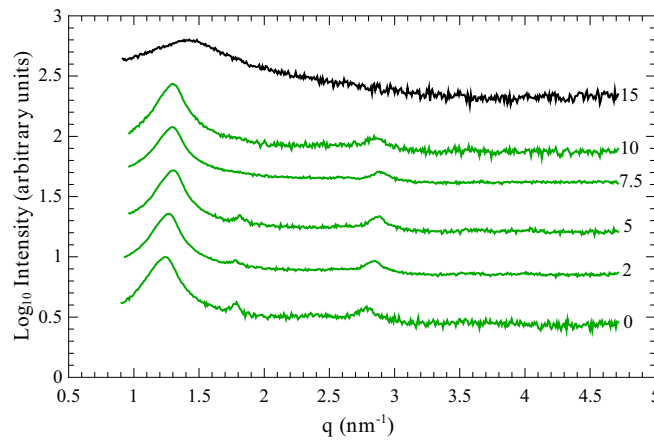

FIG. 8. SAXS patterns showing the effect of osmotic pressure on S_I^c; $\rho = 2$, [CTAT] = 100 mM. Numbers against the curves indicate the concentration of PVP10 000 in the solution. Peaks in the scattering patterns can be indexed following the scheme $q_{hk} \propto \sqrt{h^2 + k^2}$.

APPENDIX C: OSMOTIC PRESSURE OF PEG8000 AND PVP10 000 SOLUTIONS

See the osmotic pressure data presented in Table IV.

TABLE IV. Osmotic pressure (π) applied by solutions of neutral polymers PEG8000 and PVP10 000 for a few concentrations. (taken from Ref. [30]).

PEG 8000		PVP 10 000	
wt %	π (10^5 Pa)	wt %	π (10^5 Pa)
0	0	0	0
5	0.39	5	3.55
10	1.33	7.5	4.68
15	3.12	10	5.37
20	6.12	15	7.01

[1] G. S. Manning, J. Chem. Phys. **51**, 924 (1969).

[2] M. L. Bret and B. H. Zimm, Biopolymers **23**, 287 (1984).

[3] D. P. Mascotti and T. M. Lohman, Proc. Natl. Acad. Sci. USA **87**, 3142 (1990).

[4] K. Wagner, D. Harries, S. May, V. Kahl, J. O. Rädler, and A. Ben-Shaul, Langmuir **16**, 303 (2000).

[5] C. E. Sing, Adv. Colloid Interface Sci. **239**, 2 (2017).

[6] J. O. Rädler, I. Koltover, T. Salditt, and C. R. Safinya, Science **275**, 810 (1997).

[7] D. D. Lasic, H. Strey, M. C. A. Stuart, R. Podgornik, and P. M. Frederik, J. Am. Chem. Soc. **119**, 832 (1997).

[8] I. Koltover, T. Salditt, J. O. Rädler, and C. R. Safinya, Science **281**, 78 (1998).

[9] F. Artzner, R. Zantl, G. Rapp, and J. O. Rädler, Phys. Rev. Lett. **81**, 5015 (1998).

[10] H. M. Evans, A. Ahmad, K. Ewert, T. Pfohl, A. Martin-Herranz, R. F. Bruinsma, and C. R. Safinya, Phys. Rev. Lett. **91**, 075501 (2003).

[11] R. Krishnaswamy, P. Mitra, V. A. Raghunathan, and A. K. Sood, Europhys. Lett. **62**, 357 (2003).

[12] J. DeRouchey, R. R. Netz, and J. O. Rädler, Euro. Phys. J. E: Soft Matter Biol. Phys. **15**, 17 (2005).

[13] A. V. Radhakrishnan, S. K. Ghosh, G. Pabst, V. A. Raghunathan, and A. K. Sood, Proc. Natl. Acad. Sci. USA **109**, 6394 (2012).

[14] P. L. Felgner, T. R. Gadek, M. Holm, R. Roman, H. W. Chan, M. Wenz, J. P. Northrop, G. M. Ringold, and M. Danielsen, Proc. Natl. Acad. Sci. USA **84**, 7413 (1987).

[15] P. L. Felgner and G. Rhodes, Nature (London) **349**, 351 (1991).

[16] R. Bruinsma, Euro. Phys. J. B **4**, 75 (1998).

[17] S. May, D. Harries, and A. Ben-Shaul, Biophys. J. **78**, 1681 (2000).

[18] D. Danino, E. Kesselman, G. Saper, H. I. Petrache, and D. Harries, Biophys. J. **96**, L43 (2009).

[19] R. Krishnaswamy, G. Pabst, M. Rappolt, V. A. Raghunathan, and A. K. Sood, Phys. Rev. E **73**, 031904 (2006).

[20] F. A. Soltero, J. E. Puig, O. Manero, and P. C. Shulz, Langmuir **11**, 3337 (1995).

[21] M. E. Cates and S. J. Candau, J. Phys.: Condens. Matter **2**, 6869 (1990).

[22] A. Pal, R. Mary, and V. A. Raghunathan, J. Mol. Liq. **174**, 48 (2012).

[23] V. K. Aswal and P. S. Goyal, Phys. Rev. E **61**, 2947 (2000).

[24] D. M. LeNevue and R. Rand, Biophys. J. **18**, 209 (1977).

[25] R. P. Rand and V. A. Parsegian, Biochim. Biophys. Acta **988**, 351 (1989).

[26] M. Dubois, T. Zemb, L. Belloni, A. Delville, P. Levitz, and R. Setton, J. Chem. Phys. **96**, 2278 (1992).

[27] J. C. Wang, Proc. Natl. Acad. Sci. USA **76**, 200 (1979).

[28] V. Lorman, R. Podgornik, and B. Žekš, Phys. Rev. Lett. **87**, 218101 (2001).

[29] I. Kamal, A. K. Das, P. S. Goyal, and G. U. Ahmad, Bangladesh Journal Physics **15**, 105 (2014).

[30] https://scholars.huji.ac.il/danielharries/book/osmotic-stress-data.